

Structural and luminescent properties of ZnTe film grown on silicon by metalorganic chemical vapor deposition

C. X. Shan, X. W. Fan, J. Y. Zhang, Z. Z. Zhang, X. H. Wang et al.

Citation: *J. Vac. Sci. Technol. A* **20**, 1886 (2002); doi: 10.1116/1.1507344

View online: <http://dx.doi.org/10.1116/1.1507344>

View Table of Contents: <http://avspublications.org/resource/1/JVTAD6/v20/i6>

Published by the AVS: Science & Technology of Materials, Interfaces, and Processing

Related Articles

Enhanced green emission from UV down-converting Ce³⁺-Tb³⁺ co-activated ZnAl₂O₄ phosphor
J. Vac. Sci. Technol. B **30**, 031401 (2012)

Characterization of epitaxial ZnTe layers grown on GaAs substrates by transmission electron microscopy and photoluminescence
J. Vac. Sci. Technol. A **30**, 021508 (2012)

Photoluminescence and secondary ion mass spectrometry study of layer-by-layer grown Zn_{1-x}Cd_xSe quantum wells
J. Vac. Sci. Technol. B **29**, 03C137 (2011)

Anomalous optical processes in photoluminescence from ultrasmall quantum dots of ZnO
J. Vac. Sci. Technol. A **29**, 03A120 (2011)

Strong enhancement of ultraviolet emission from ZnO films by V implantation
J. Vac. Sci. Technol. B **29**, 021207 (2011)

Additional information on *J. Vac. Sci. Technol. A*

Journal Homepage: <http://avspublications.org/jvsta>

Journal Information: http://avspublications.org/jvsta/about/about_the_journal

Top downloads: http://avspublications.org/jvsta/top_20_most_downloaded

Information for Authors: http://avspublications.org/jvsta/authors/information_for_contributors

ADVERTISEMENT



Aluminum Valves with Conflat® Flanges

Less Outgassing Than Stainless
Mate to Stainless Steel Conflats
Sizes From 2.75 to 14 inch O.D.
Leak Rate Less Than 10⁻¹⁰ SCC/S

Visit us
at Booth # 300
in Tampa

Prices & Specifications
vacuumresearch.com



Structural and luminescent properties of ZnTe film grown on silicon by metalorganic chemical vapor deposition

C. X. Shan,^{a)} X. W. Fan, J. Y. Zhang, Z. Z. Zhang, X. H. Wang,^{b)} J. G. Ma, Y. M. Lu, Y. C. Liu, D. Z. Shen, X. G. Kong, and G. Z. Zhong

Key Laboratory of Excited State Processes, Changchun Institute of Optics, Fine Mechanics and Physics, Chinese Academy of Sciences, No. 140 Ren Min Street, Changchun 130022, People's Republic of China

(Received 29 January 2002; accepted 22 July 2002)

Reported here are the structural and luminescent properties of ZnTe films grown on Si substrates by metalorganic chemical vapor deposition (MOCVD). ZnO intermediate layers annealed at different temperature are employed to buffer the thermal and chemical difference between the ZnTe epilayers and silicon substrates. With increasing the annealing temperature of ZnO buffer layer, the crystallization of ZnTe assessed by x-ray diffraction is improved. Temperature dependent photoluminescence (PL) of the ZnTe epilayer is processed to evaluate the optical properties of our samples. The PL spectra are characterized by an asymmetry line shape labeled *E*, and it can be dissolved into two Gaussian lines with energy discrepancy of about 18.5 meV. The origins of these two Gaussian lines are thought to be free and bound excitons emission, respectively. The dependence of luminescence on temperature indicates that the emission from bound excitons dominates the spectrum below 157 K. While above 157 K, the bound excitons are detrapped to become free excitons, and free excitons emission becomes dominant. Also, the broadening of the emission line resulting from the ionized impurity scattering cannot be neglected above 157 K. Temperature dependence of the full width at half maximum and peak energy of the spectra can be comprehended well under the framework of the two-dissociation-process theory, which, in turn, further strengthens the validity of the origin of the spectra. © 2002 American Vacuum Society. [DOI: 10.1116/1.1507344]

I. INTRODUCTION

In the past few years, considerable attention has been paid to the growth of II–VI group semiconductors. This attention stems both from the fundamental interest in these compounds and from their potential practical applications when incorporated within electronic and optoelectronic devices.^{1–3} As an important material in modern semiconductor technology, silicon has served electronics well. It has such advantages as high thermal and electrical conductivity, high crystal and surface quality and also a mature technology for preparing cheap, large-area, dislocation-free wafers. Those strong points make this material advantageous in numerous applications in microelectronics. The possibilities of integrating the optoelectronics based on semiconductors with Si-base microelectronics motivate enormous interest and effort to study the growth of II–VI group semiconductors on Si substrates. However, the large difference in thermal and chemical properties between most semiconductor materials and silicon inhibits heteroepitaxial of II–VI group semiconductors on silicon.^{4,5} Furthermore, the poor wetting of the polar compounds on nonpolar silicon substrates impedes the direct nucleation and consequently results in poor quality and morphology of the epilayer. Adding a zinc oxide (ZnO) buffer

layer between the epilayer and Si substrate can be one promising way to overcome the abovementioned inconveniences.

In this article, the structural and luminescent properties of ZnTe film on Si (111) substrates, employing ZnO as a buffer layer are studied. The thermal expansion coefficients of ZnTe, ZnO, and silicon are 8.3×10^{-6} , 5.5×10^{-6} , and $2.44 \times 10^{-6} \text{ K}^{-1}$, respectively. One can see that the thermal expansion coefficient of ZnO is almost the mean value between those of ZnTe and silicon. Therefore, the ZnO layer can lessen the thermal stress between ZnTe epilayer and Si substrate. Second, the surface of the Si wafer may be covered by a thin SiO_x film,⁶ which has better wetting properties with the ZnO layer. Third, ZnO is a proven buffer layer.⁷ The abovementioned facts provide a solid ground for the growth of ZnTe film on ZnO buffered silicon substrate.

II. EXPERIMENTAL PROCEDURE

The preparation of the samples was performed by a magnetron driven sputtering and low-pressure metalorganic chemical vapor deposition (MOCVD) technique. Prior to the growth, the Si (111) wafers were cleaned according to the method depicted in previous literature.⁸ The growth procedure progressed in two steps: first sputter ZnO layer with thickness of about $0.8 \mu\text{m}$ at 150°C in the gas mixture of Ar (75%) and O_2 (25%) by a radio frequency magnetron driven sputtering equipment. After that, the ZnO layer was annealed in oxygen ambient for 1 h. A ZnTe layer with the thickness of 800 nm was then deposited onto the ZnO coated Si (111) substrate by MOCVD at 420°C with the growth pressure of

^{a)} Author to whom correspondence should be addressed; electronic mail: shen@public.cc.jl.cn

^{b)} Also at National Key Laboratory of High Power Semiconductor Laser, Changchun Institute of Optics and Fine Mechanics, No. 7 WeiXing Road, Changchun 130022, People's Republic of China.

TABLE I. The growth conditions of ZnTe films.

	Sample A	Sample B	Sample C	Sample D	Sample E
Structure	ZnTe/ZnO/Si	ZnTe/ZnO/Si	ZnTe/ZnO/Si	ZnTe/ZnO/Si	ZnTe/ZnO/Si
Annealing temperature of ZnO (°C)	No annealing	600	700	800	900

220 mm Hg. Dimethylzinc (DMZn) and diethyltelluride (DETe) were employed as sources of Zn and Te. A series of samples with different annealing duration of ZnO layer were prepared by the abovementioned procedure. Table I shows the detailed growth conditions of our samples. The structural properties of the samples were accessed by a *D/max-rA* x-ray diffraction (XRD) spectrometer (Rigaku) with a $\text{Cu } K\alpha$ line of 1.54 Å. The luminescent properties were characterized by photoluminescence (PL) spectra. The 488 nm line of an Ar^+ laser was used as the excitation source and the signals were recorded by the charge-coupled device (CCD) of a JY-630 micro-Raman spectrograph designed specially for wide band gap semiconductors.

III. RESULTS AND DISCUSSION

A. Structural properties of ZnTe film

Figure 1 shows the x-ray diffraction patterns of the five samples mentioned in Table I. For comparison, the diffraction pattern of the ZnTe film grown on the bare Si (111) substrate is shown in the inset. As displayed in the figure, although all five samples show polyorientation, they are all preferred ZnTe (111) oriented. The lattice constant of the

ZnTe film calculated from the XRD patterns is $a_{\text{ZnTe}} = 6.092 \text{ \AA}$, which is closely consistent with the value of 6.101 Å reported in the literature.⁹ With increasing the annealing temperature, the full width at half maximum (FWHM) of ZnTe (111) decreases. At the same time, the sum intensity ratio of $I_{\text{ZnTe}(111)}$ and $I_{\text{ZnTe}(222)}$ to that of the whole ZnTe diffraction peaks, which reflects the crystallization of ZnTe layer somewhat, increases from 0.957 to 0.995 as the annealing temperature of ZnO layer goes up from 600 to 900 °C, as shown in Table II. Given that the sum ratio of $I_{\text{ZnTe}(111)}$ and $I_{\text{ZnTe}(222)}$ to that of the whole ZnTe diffraction peaks of the ZnTe deposited directly onto Si (111) substrate is only 0.777. One can conclude that the crystallization of ZnTe layers is greatly enhanced because of the ZnO buffer layer. Moreover, by increasing the annealing temperature of the ZnO buffer layer, the crystallization of ZnTe films is improved further.

B. Luminescent properties of ZnTe film

The PL spectrum of sample E at 83 K was shown in Fig. 2. Three distinct peaks appear in the spectrum and are labeled *E*, I_1 , and I_2 , respectively. The enlarged *E* was shown

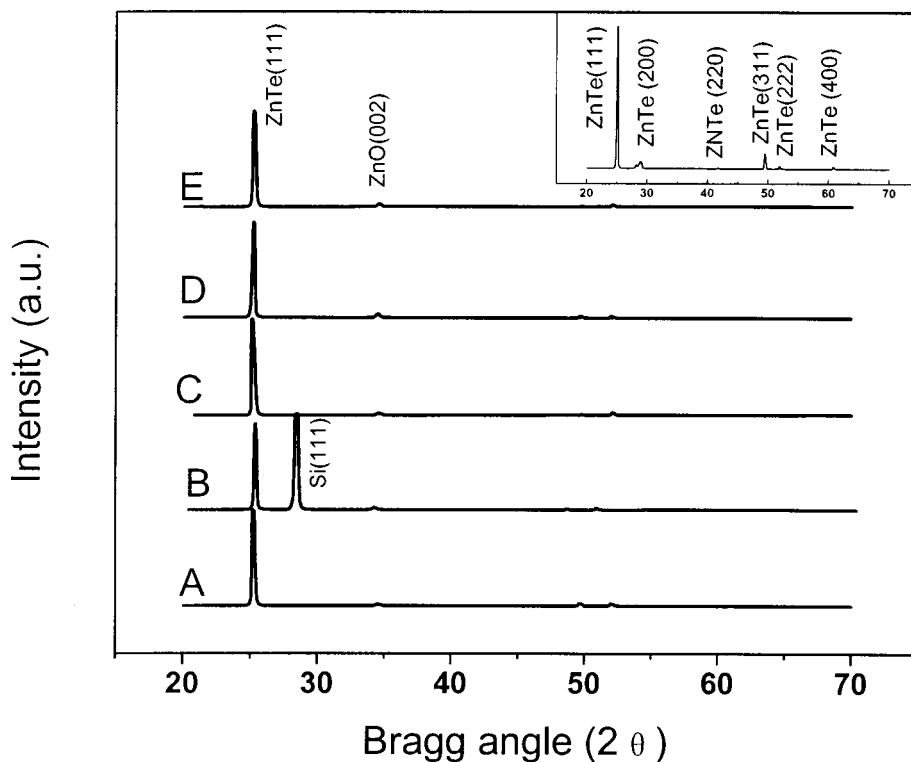


FIG. 1. X-ray diffraction patterns of ZnTe/ZnO/Si structures under different annealing temperature of ZnO buffer layer in pure oxygen for 1 h. (A) No annealing; (B) 600 °C; (C) 700 °C; (D) 800 °C; (E) 900 °C. The inset shows the XRD pattern of ZnTe film grown directly onto silicon substrate.

TABLE II. Statistical results of the five samples mentioned in Table I.

	Sample A	Sample B	Sample C	Sample D	Sample E
FWHM of ZnTe (111) (deg)	0.429	0.413	0.322	0.287	0.286
$I_{(111)+(222)}/I_{\text{total}}$	0.957	0.972	0.972	0.974	0.995

in the inset of the figure. The emission line can be decomposed into two Gaussian lines marked FE and BE, respectively. The ionization energy of the persistent donor in ZnTe is about 18.3 meV,¹⁰ which is consistent with the 18.5 meV of the energy difference between FE and BE. We attribute FE and BE to emissions from free excitons and excitons bound to neutral donors, respectively. The temperature dependence photoluminescence detailed hereafter verified the assignment further. As for I_1 and I_2 , they vanish rapidly as temperature rises, which is similar to the characters of impurity-related transitions.¹¹ Therefore, they may be the unidentified impurity-related transitions, and the real origins need to be further investigated.

1. Temperature dependence of emission intensity

Figure 3 illustrates the dependence of the PL spectra and the integrated intensity of peak E on inverse temperature. As shown in the figure, two distinct temperature regions appear, one is in the range from 83 to 157 K, and the other from 157 to 300 K. The solid curve is the theoretically fit to the integrated PL intensity (I_{PL}) using the following equation:^{12–14}

$$I(T) = \frac{I_0}{1 + A_1 \exp\left(\frac{-E_1}{K_B T}\right) + A_2 \exp\left(\frac{-E_2}{K_B T}\right)}, \quad (1)$$

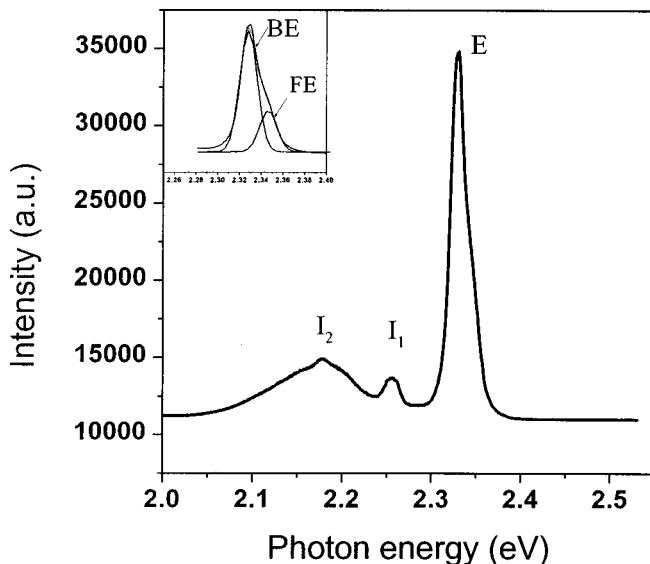


Fig. 2. Typical photoluminescence spectrum of sample E at 83 K. The inset displays the enlarged lineshape of peak E.

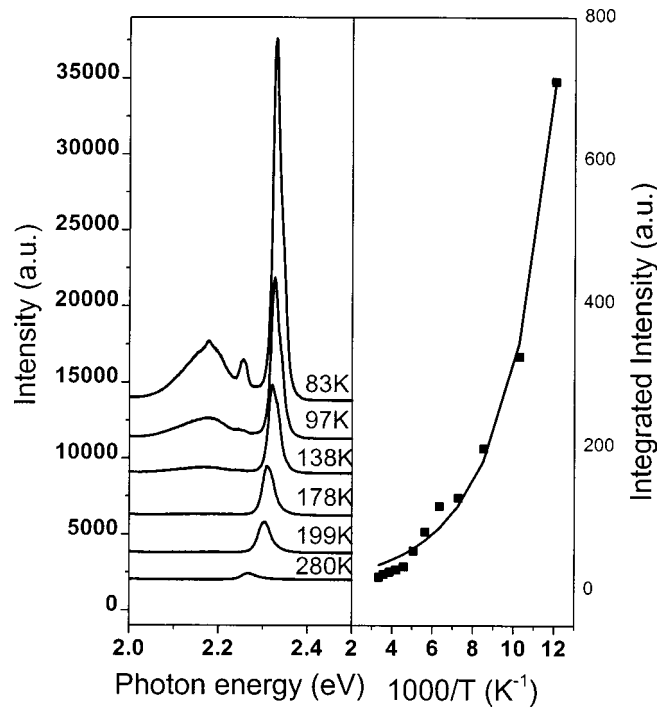


Fig. 3. Left-hand side: The side PL spectra of sample E at different temperature. Right-hand side: Arrhenius plot of the integrated intensity of peak E vs inverse temperature. The curve is the fit to the scattered experimental data using the following expression: $I(T) = I_0 [1 + A_1 \exp(-E_1/K_B T) + A_2 \exp(-E_2/K_B T)]^{-1}$.

where I_0 , A_1 , and A_2 are constants, T is the sample temperature, K_B is Boltzmann constant, E_1 and E_2 are the activation energies. By plotting $I(T)$ vs $1000/T$, two activation energies are derived, $E_1 = 13.6$ and $E_2 = 19.3$ meV. Noting that the activation energy obtained in this way is usually considered as the total binding energy, which includes the confinement energy and the exciton binding energy.¹⁵ The grain size of our sample is in the micron scale. Comparing the exciton binding energy, the confinement energy is negligible. Since the binding energy of the free exciton in ZnTe is 12 meV,¹¹ which is close to the value of E_1 , one can deduce that E_1 corresponds to the dissociation of free excitons. Since E_2 is almost equal to the ionized energy of persistent donor in ZnTe, it can be judged to be the activation energy of the donor. These results, in turn, verify that E is the combination emission of the free excitons and bound excitons. In the low temperature range, 83–157 K, the emission from BE governs the emission of E . With increasing temperature, the BE will detrapp to become free excitons, and the emission from free excitons becomes dominant in temperature range from 157 to 300 K.

2. Temperature dependence of FWHM

The dependence of FWHM of peak E on temperature is shown in Fig. 4, in which, the scattered rectangles are the experimental data, and the curves indicate the simulation to the data. As illustrated by the experimental data, the line-

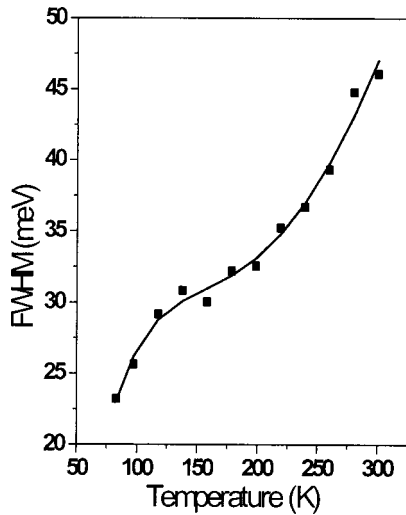


FIG. 4. Temperature dependence of the linewidth (FWHM) of peak E. The rectangles show the experimental data and the curve is obtained by fitting the experimental data using Eq. (2).

width increases with temperature. However, there is a kink point at about 157 K, which is taken to originate from the impurity scattering, as detailed hereafter.

In general, the FWHM of an emission line is mainly contributed to by an inhomogeneous component (Γ_{inh}) and a temperature-dependent homogeneous component (Γ_h). The inhomogeneous part of Γ_{inh} mainly results from the nonuniformity in the epilayer, while the homogeneous component comprise three parts.¹⁶ At low temperature, the scattering by longitudinal acoustic (LA) phonon dominates the broadening of the emission. At moderate temperatures, scattering by the longitudinal optical (LO) phonon becomes dominant due to the increase of the phonon population. As the temperature increases further (> 157 K in our experiment), the broadening due to impurity scattering must be taken into account because of the ionization of some impurities. Based on the above depiction, the FWHM can be expressed as follow:¹⁷⁻¹⁹

$$\Gamma = \Gamma_{inh} + \Gamma_{LA}T + \frac{\Gamma_{LO}}{\exp(E_{LO}/K_B T) - 1} + \frac{\Gamma_{imp}}{\exp(E_{imp}/K_B T)}, \quad (2)$$

where Γ_{inh} is the inhomogeneous broadening factor, Γ_{LA} , Γ_{LO} , and Γ_{imp} are the measure weightings of the LA, LO phonon and impurity scattering, respectively. E_{LO} is the energy of LO phonon and E_{imp} is the ionization energy of impurity. K_B is the Boltzmann constant and T is the sample temperature. Given that the LO phonon energy in ZnTe is 26.1 meV,²⁰ by fitting the experimental data in Fig. 4, as shown by the curve in the figure, one can get $E_{LO} = 25.7$ meV and $E_{imp} = 17.4$ meV. The accordance of E_{LO} to the LO phonon energy and E_{imp} to the ionization energy of the persistent donor in ZnTe strengthen the identification of the origin of peak E further.

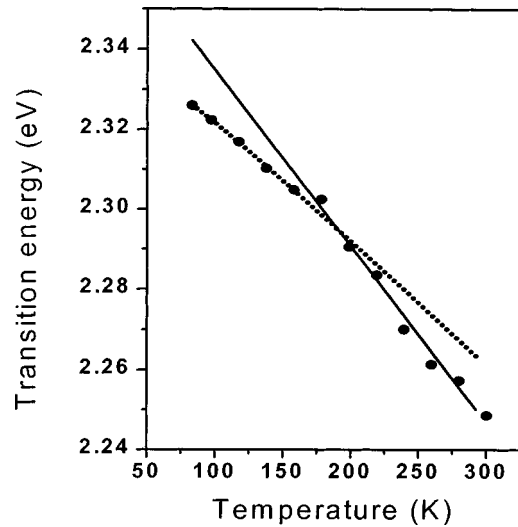


FIG. 5. Temperature dependence of the peak energy of peak E. The dotted line shows the fit to the experimental data from 83 to 157 K and the solid line indicates the fit to the data from 157 to 300 K using Varshni equation.

3. Temperature dependence of peak energy

The dependence of the peak energy of peak E on temperature is displayed in Fig. 5. The solid circles denote experimental data and the solid line indicates a theoretical fit to the empirical data using the Varshni equation:²¹

$$E_g(T) = E_g(0) - \frac{\alpha T^2}{T + \beta}, \quad (3)$$

where $E_g(0)$ is the peak energy at 0 K, α and β are constants and T is the temperature. Since the emission spectra in our experiment exhibit distinct two-temperature-region character, we simulate the data in Fig. 5 in two regions accordingly. By fitting the experimental data from 83 to 157 K, we get $E_g(0) = 2.363$ eV. In the same way the value of $E_g(0)$ obtained by fitting the data from 157 to 300 K is 2.379 eV, which is in little difference with the reported band gap of ZnTe at 0 K considering the exciton binding energy.²² The energy discrepancy between the two $E_g(0)$ s is 15.1 meV, which is, taking into account the error, close to the energy difference of free excitons and bound excitons. Moreover, temperature coefficient of the peak energy obtained from fitting above 157 K is 4.4×10^{-4} eV/K, which is almost same to the reported 4.5×10^{-4} eV/K in ZnTe.¹⁷ This, again, agrees with the results discussed above.

IV. CONCLUSIONS

In conclusion, ZnTe films are prepared on silicon substrate with a ZnO buffer layer by MOCVD. The structural properties of the ZnTe layer evaluated by x-ray diffraction indicate that with increasing the annealing temperature, the crystallization of the ZnTe film is improved. The optical properties have been investigated by temperature-dependent PL measurement. The PL spectrum is characterized by an asymmetry line shape labeled E in the temperature range from 83 to 300 K, and it can be decomposed into two Gauss-

ian lines with an energy discrepancy of about 18.5 meV. The origin of E is thought to be the recombination of free and bound excitons. The dependence of luminescence intensity on temperature indicates, at about 157 K, the bound excitons are detrapped to become free excitons and free exciton emissions becomes dominant above 157 K. Also, the temperature dependence of FWHM and peak energy of peak E validate the origin of peak E.

ACKNOWLEDGMENTS

This research is supported by the National Fundamental and Applied Research Project; The Key Project of the National Natural Science Foundation of China, No. 69896260; The Innovation Project Item, Chinese Academy of Sciences; The Program of CAS Hundred Talents; The National Natural Science Foundation of China and the “863” Advanced Technology Research Program.

¹Y. Luo, S. P. Guo, O. Maksimov, M. C. Tamargo, V. Asnin, F. H. Pollak, and Y. C. Chen, *Appl. Phys. Lett.* **77**, 4259 (2001).

²M. Klude and D. Hommel, *Appl. Phys. Lett.* **79**, 2523 (2001).

³J. Gu, K. Tonomura, N. Yoshikawa, and T. Sakaguchi, *J. Appl. Phys.* **44**, 4692 (1973).

⁴L. T. Romano, R. D. Bringans, X. Zhou, and W. P. Kirk, *Phys. Rev. B* **52**, 11201 (1995).

⁵V. H. Méndez-García, A. Pérez Centeno, M. López-López, M. Taamura, K. Momose, K. Ojima, and H. Yonezu, *Thin Solid Films* **373**, 33 (2000).

⁶A. Ishizaka and Y. Shiraki, *J. Electrochem. Soc.* **133**, 666 (1986).

⁷T. Detchprohm, H. Amano, K. Hiramatsu, and I. Akasaki, *J. Cryst. Growth* **128**, 384 (1993).

⁸C. X. Shan, X. W. Fan, J. Y. Zhang, Z. Z. Zhang, J. G. Ma, Y. M. Lu, Y. C. Liu, and D. Z. Shen, *J. Cryst. Growth* **233**, 795 (2001).

⁹B. L. Sharma and R. K. Purohit, *Semiconductor Heterojunctions* (Pergamon, New York, 1974), p. 24.

¹⁰J. L. Pautrat, J. M. Francou, N. Magnea, E. Molva, and K. Saminadayar, *J. Cryst. Growth* **72**, 194 (1985).

¹¹A. Naumov, K. Wolf, T. Reisinger, H. Stanzl, and W. Gebhardt, *J. Appl. Phys.* **73**, 2581 (1993).

¹²D. Bimberg, M. Sondergeld, and E. Grobe, *Phys. Rev. B* **4**, 3451 (1971).

¹³Y.-H. Wu, K. Arai, and T. Yao, *Phys. Rev. B* **53**, R10485 (1996).

¹⁴S. Iyer, S. Hegde, A. Abul-Fradl, K. K. Bajaj, and W. Mitchel, *Phys. Rev. B* **47**, 1329 (1993).

¹⁵S. Weber, W. Limmer, K. Thonke, R. Sauer, K. Panzlaff, G. Bacher, H. P. Meier, and P. Roentgen, *Phys. Rev. B* **52**, 14739 (1995).

¹⁶S. Z. Wang, S. F. Yoon, L. He, and X. C. Shen, *J. Appl. Phys.* **90**, 2314 (2001).

¹⁷S. Yoshimura, H. Nakata, T. Ohyama, E. Otsuka, J. Li, and S. Yuan, *Jpn. J. Appl. Phys., Part 1* **34**, 1459 (1995).

¹⁸H. J. Lozykowski and V. K. Shastri, *J. Appl. Phys.* **69**, 3235 (1991).

¹⁹T. Li, H. J. Lozykowski, and J. L. Reno, *Phys. Rev. B* **46**, 6961 (1992).

²⁰H. Venghaus and P. J. Dean, *Phys. Rev. B* **21**, 1596 (1980).

²¹Y. P. Varshni, *Physica (Amsterdam)* **34**, 149 (1967).

²²R. E. Nahory and H. Y. Fan, *Phys. Rev. Lett.* **17**, 251 (1966).